Supporting Information for:

Probing the Origins of Catalytic Discrimination Between Phosphate and Sulfate Monoester Hydrolysis: Comparative Analysis of Alkaline Phosphatase and Protein Tyrosine Phosphatases

Logan D. Andrews[a], Jesse G. Zalatan[b], and Daniel Herschlag[c,*]

[a]Department of Chemical and Systems Biology, [b]Department of Chemisty, and [c]Department of Biochemistry, Stanford

[*]Corresponding author:
Dept. of Biochemistry, B400
Stanford University
Stanford, CA 94305-5307
650-723-9442 (telephone)
650-723-6783 (fax)
herschla@stanford.edu

Table S1. Kinetic Parameters and Discrimination of Phosphate versus Sulfate Monoester Hydrolysis by AP Superfamily Members and PTPs

	k_{cat} (s^{-1})		K_M (M^{-1})		k_{cat}/K_M ($M^{-1}s^{-1}$)		rate enhancement[a]		discrimination[b]
	*p*NPP	*p*NPS	*p*NPP	*p*NPS	*p*NPP	*p*NPS	*p*NPP	*p*NPS	
AP[c]									
WT[d]	12	-	4×10^{-7}	-	3.3×10^{7} *(5.8×10^{8})*	2.8×10^{-3}	7×10^{17} (1×10^{19})	3×10^{8}	2×10^{9} (3×10^{10})
D153A	5.6	-	2.0×10^{-6}	-	2.8×10^{6}	6.3×10^{-4}	6×10^{16}	7×10^{7}	9×10^{8}
D153A/R166S	7.0×10^{-2}	-	5.3×10^{-6}	-	1.3×10^{4}	3.0×10^{-5}	2×10^{14}	3×10^{6}	7×10^{7}
E322Y[e]	3.6×10^{-3}	-	$\sim5\times10^{-7}$	-	7.2×10^{3}	2.9×10^{-6}	1×10^{14}	3×10^{5}	3×10^{8}
R166S[e]	0.50	-	5.0×10^{-6}	-	1.0×10^{5}	6.8×10^{-5}	2×10^{15}	8×10^{6}	3×10^{8}
R166S/E322Y[e]	4.3×10^{-5}	-	2.7×10^{-5}	-	1.6	$\leq10^{-6}$	3×10^{10}	$\leq1\times10^{5}$ *(1×10^{4})*	$\geq3\times10^{5}$ *(3×10^{6})*
PafA[f]	64	-	1.1×10^{-4}	-	5.8×10^{5}	4.9×10^{-4}	1×10^{16}	5×10^{7}	2×10^{8}
PAc[g]	0.2	$\sim2\times10^{-7}$	1.4×10^{-2}	1×10^{-2}	20	$\sim2\times10^{-5}$	4×10^{11}	2×10^{6}	2×10^{5}
NPP[h]	-	-	-	-	1.1	2.0×10^{-5}	2×10^{10}	2×10^{6}	1×10^{4}
PMH[i]	7.7×10^{-3}	4.0×10^{-2}	3.5×10^{-4}	6.8×10^{-2}	22	0.59	2×10^{11}	3×10^{10}	7
PAS[j]	2.3×10^{-2}	14	2.9×10^{-5}	2.9×10^{-7}	790	4.9×10^{7}	2×10^{13}	5×10^{18}	4×10^{-6}
PTP[k]									
Stp1	7	4.4×10^{-7}	2.7×10^{-4}	8×10^{-3}	2.6×10^{4}	5.5×10^{-5}	2×10^{14}	3×10^{6}	7×10^{7}
PTP1B	210	2.3×10^{-5}	2.3×10^{-3}	2×10^{-2}	9.3×10^{4}	1.1×10^{-3}	8×10^{14}	6×10^{7}	1×10^{7}
Yop$^{51*}\Delta$162	250	1.1×10^{-5}	1.6×10^{-3}	4×10^{-3}	1.6×10^{5}	3.2×10^{-3}	1×10^{15}	2×10^{8}	5×10^{6}

'-' indicates not measurable: The *p*NPS hydrolysis activity of WT AP, AP mutants, and PafA remains first-order in *p*NPS substrate concentration up to ~40 mM *p*NPS and thus, values for k_{cat} and K_M cannot be obtained. [a] Rate enhancement = $(k_{cat}/K_M)/(k_w)$; k_w is the second-order rate constant for attack of water on the monoester. The k_w value for *p*NPP hydrolysis was determined[1] at 39 °C and corrected to 25 °C (5×10^{-11} $M^{-1}s^{-1}$), the temperature at which the AP assays were conducted, and 30 °C (1×10^{-10} $M^{-1}s^{-1}$), the temperature at which the PTP assays were conducted, using the reported temperature dependence.[1] The k_w value for *p*NPS hydrolysis at 25 °C (9×10^{-12} $M^{-1}s^{-1}$) and 30 °C (1.7×10^{-11} $M^{-1}s^{-1}$) was corrected from the value[2] at 35 °C by using the reported temperature dependence.[2] [b] Discrimination = (rate enhancement *p*NPP)/(rate enhancement *p*NPS). [c] Kinetic assays for WT AP and mutants were conducted in 100 mM NaMOPS, pH 8.0, 100 mM NaCl, 1 mM $MgCl_2$, and 100 μM $ZnCl_2$ at 25 °C. [d] The rate constant for WT AP *p*NPP hydrolysis[3] was used to estimate the expected second-order rate constant shown in parenthesis for the enzymatic reaction if the chemical step rather than diffusion was rate-limiting as described in Text S1. The rate constant for WT AP *p*NPS hydrolysis was measured here using a discontinuous assay (see Methods) and is good agreement with the previously published value using a continuous assay.[4] [e] Values for E322Y and R166S/E322Y AP are from [5]. The value for R166S AP is from [6]. The rate constant measured for R166S/E322Y AP *p*NPS hydrolysis activity is an upper limit and the value in parenthesis is the expected value if the effects on activity of the

R166S and E322Y mutations are additive. This value was not included in Figure 6. [f] PafA[7] is a two-metal phosphate monoesterase of the AP superfamily.[7] Kinetic measurements were conducted in 100 mM Tris•HCl, pH 8.0, 0.5 M NaCl, and 100 μM $ZnCl_2$ at 25 °C. [g] PAc = Phosphonoacetate hydrolase. Kinetic measurements were conducted in 100 mM Tricine, pH8.0, and 1 mM $ZnCl_2$ at 25 °C.[8] [h] NPP = Nucleotide Pyrophosphatase/Phosphodiesterase. Kinetic measurements were conducted in 100 mM MES, pH 6.5, 0.5 M NaCl, and 100 μM $ZnCl_2$ at 25 °C.[6] [i] PMH = Phosphonate monoester hydrolyase. Kinetic measurements were conducted in 44 mM NaSuccinate, pH 7.5, 33 mM imidazole, and 33 mM diethanolamine at 30 °C.[9] [j] PAS = *Pseudomonas aeruginosa* arylsulfatase. Kinetic measurements were conducted in 100 mM Tris, pH 8.0 at 25 °C.[10] [k] Kinetic measurements for PTPs were conducted in 20 mM NaMaleate, pH 6.0, 0.1 mM EDTA, and 0.15 M NaCl at 30 °C.

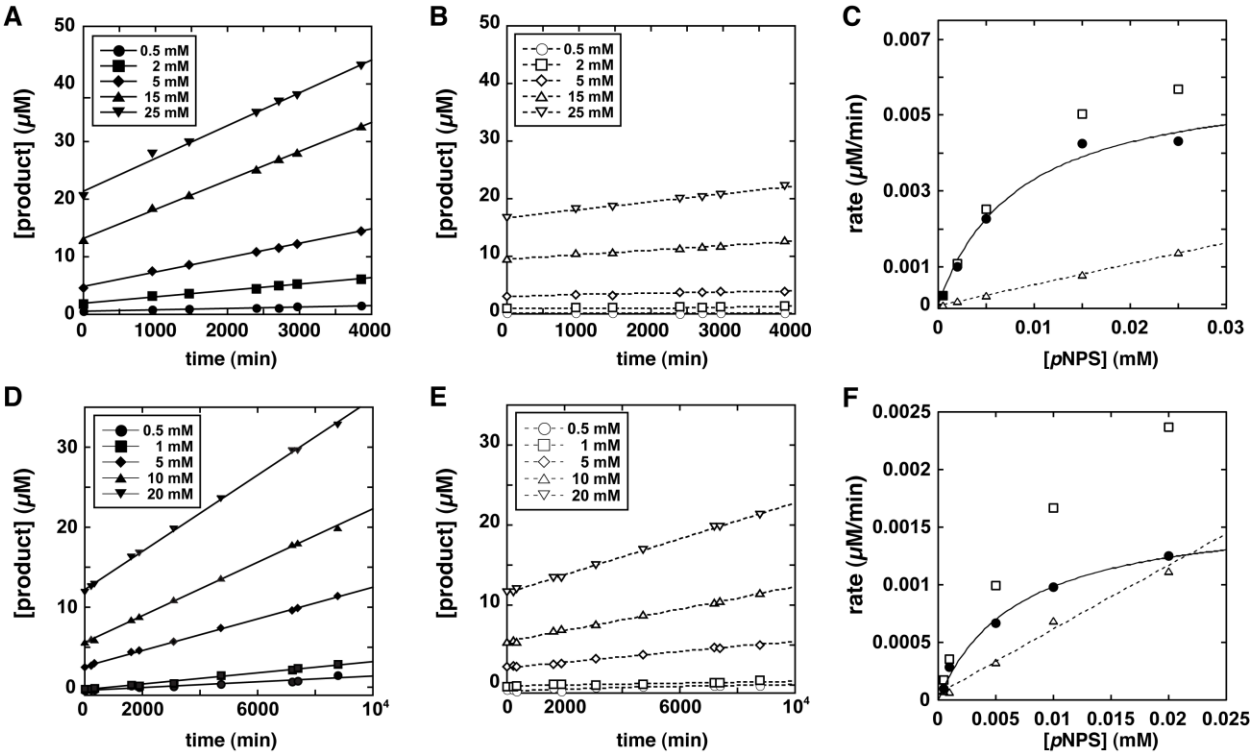

Figure S1. Kinetics for PTP Stp1 hydrolysis of *p*NPS with 230 μM (A-C) and 90 μM (D-F) Stp1. See Methods for assay conditions. (A) The increase in *p*-nitrophenolate ([product]) over time for samples containing Stp1 with various concentrations of substrate *p*NPS (various closed symbols; *p*NPS concentrations are listed within the figure panel). (B) Uncatalyzed appearance of *p*-nitrophenolate over time for samples without Stp1. (C) Plot of the observed rates with (open squares; from (A)) and without (open triangles; from (B)) Stp1 and the background-subtracted rate that represented the Stp1-catalyzed reaction (closed cirlces). The background rates gave a linear fit as expected for the nonenzymatic hydrolysis of *p*NPS by water and a second-order rate constant for uncatalyzed *p*NPS hydrolysis of 1.7×10^{-11} $M^{-1}s^{-1}$ that agrees with a previous measurement under similar conditions.[11] The Stp1-catalyzed reaction followed saturation kinetics (solid line) and gave values of $k_{cat} = 4.4 (\pm 0.5) \times 10^{-7}$ s^{-1}; $K_M = 8 \pm 2$ mM; and $k_{cat}/K_M = 5.5 \times 10^{-5}$ $M^{-1}s^{-1}$. (D-F) Repeat measurement of *p*NPS hydrolysis as described in parts (A-C) but with 90 μM Stp1. The Stp1-catalyzed reaction followed saturation kinetics (solid line) and gave values of $k_{cat} = 3.0 (\pm 0.3) \times 10^{-7}$ s^{-1}; $K_M = 7 \pm 2$ mM; and $k_{cat}/K_M = 4.3 \times 10^{-5}$ $M^{-1}s^{-1}$.

Text S1.

The hydrolysis activity of *p*NPP by WT AP is limited by association rather than a chemical step, as suggested by studies that probed the viscosity dependence of activity.[3,12,13] The absence of heavy-atom isotope effects for the AP-catalyzed *p*NPP hydrolysis reaction also suggests that a nonchemical step is rate-limiting for the hydrolysis of this substrate.[14] Thus, the observed k_{cat}/K_M value for the *p*NPP hydrolysis of 6.6×10^6 to 4.6×10^7 $M^{-1}s^{-1}$ [3,15,16] likely reflects the substrate binding step, and the chemical step in which the monoester bond is broken is faster than the dissociation of the substrate from the enzyme.

To estimate the rate constant for the chemical step of *p*NPP hydrolysis by AP, a comparison was made to the activity of an ethyl phosphate monoester substrate for which there is strong evidence for a rate-limiting chemical step.[3] The rate constant for hydrolysis of this substrate is 1.4×10^5 $M^{-1}s^{-1}$.[3] When Arg166, an active-site residue that makes interactions to the nonbridging oxygen atoms of the transferred phosphoryl group, is mutated to serine, the rate of ethyl phosphate hydrolysis decreases by 5800-fold to 24 $M^{-1}s^{-1}$.[17] The R166S AP hydrolysis rate constant for *p*NPP hydrolysis, which is also limited by the chemical step,[17] is 1×10^5 $M^{-1}s^{-1}$. As Arg166 likely makes the same interactions with the nonbridging oxygen atoms of the phosphoryl group for *p*NPP and ethyl phosphate, the chemical step of *p*NPP hydrolysis by WT AP is expected to be approximately 5800-fold faster compared to the hydrolysis rate constant of *p*NPP by R166S AP. This analysis predicts that if the reaction were not diffusion-limited the observed second-order rate constant for *p*NPP hydrolysis by WT AP would be 5.8×10^8 $M^{-1}s^{-1}$ [= $5800\times(1.0\times10^5$ $M^{-1}s^{-1})$, whereas the observed value of k_{cat}/K_M is 3.3×10^7 $M^{-1}s^{-1}$].[3] This calculated estimate of the second-order reaction of WT AP with *p*NPP and the uncatalyzed rate constant for

*p*NPP hydrolysis give the calculated rate enhancement for the chemical step of 10^{19}-fold and resulting discrimination of 3×10^{10} for WT AP reported in Table 1 and Table S1.

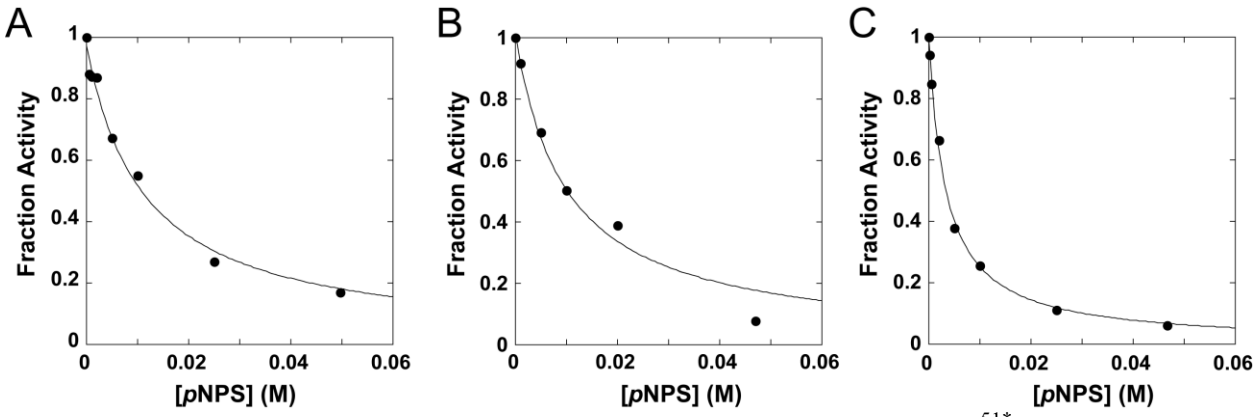

Figure S2. Catalysis of *p*NPP hydrolysis by Stp1 (A), PTP1B (B), and Yop^{51*}Δ162 (C) inhibited by *p*NPS. As the activity for the *p*NPP and *p*NPS substrates differ by more than 10^7-fold, the *p*NPS substrate does not react significantly on the time scale of the phosphatase reaction. Conditions for all assays: 20 mM NaMaleate, pH 6.0, 0.15 M NaCl, and 0.1 mM EDTA at 30 °C. The fraction of activity is plotted as a function of *p*NPS concentration. (A) For Stp1 a K_i value of 6.6 ± 0.7 mM was obtained by fitting to a competitive inhibition model. The substrate *p*NPP concentration was 200 μM and the Stp1 concentration was 200 nM. (B) For PTP 1B a K_i value of 10 ± 2 mM was obtained by fitting to a competitive inhibition model. The substrate *p*NPP concentration was 200 μM and the PTP1B concentration was 10 nM. (C) For Yop^{51*}Δ162 a K_i value of 3.1 ± 0.2 mM was obtained by fitting to a competitive inhibition model. The substrate concentration was 300 μM and the Yop^{51*}Δ162 concentration was 30 nM. The competitive inhibition by *p*NPS of *p*NPP activity corresponds to the K_M values determined for *p*NPS (Table S2), consistent with catalysis of both substrates occurring in the same active site.

Table S2. Comparison of Michaelis-Menten constants and inhibition constants for PTPs

	K_M (mM), *p*NPS[a, b]	K_i (mM), *p*NPS[a,c]
PTP		
Stp1	8 ± 2	6.6 ± 0.7
PTP1B	20 ± 6	10 ± 2
Yop^{51*}Δ162	3.5 ± 0.4	3.1 ± 0.2

[a] Values determined in 20 mM NaMaleate, pH 6.0, 0.15 M NaCl, 0.1 mM EDTA and 30 °C. [b] Values from Table S1. [c] Values from Figure S2.

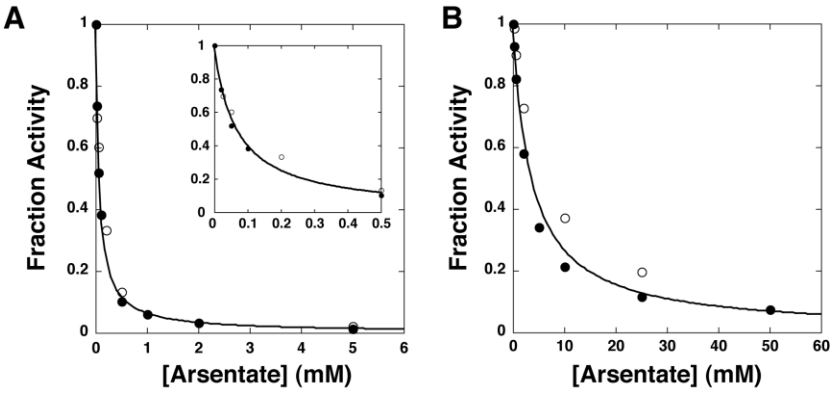

Figure S3. Inhibition of phosphatase and sulfatase reactions of PTP1B (A) and Yop^{51*}Δ162 (B) by arsenate. Observed rate constants were normalized by the observed rate in the absence of inhibitor to give the fraction activity. The lines are nonlinear least-squares fits for competitive inhibition. (A) Inhibition of PTP1B-catalyzed reactions of *p*NPP (closed circles) and *p*NPS (open circles). The values of K_i for arsenate for each reaction are 58 ± 2 μM and 82 ± 11 μM, respectively. For simplicity the combined fit to all of the data gives a value of 68 ± 5 μM (line). As the *p*NPS concentration used in the assay was near the observed K_M, which suppresses the inhibition from arsenate, we corrected for this effect using Eq. S1, which gave a value of K_i = 66 μM, in close agreement with the inhibition constant observed for the phosphatase activity. (B) Inhibition of Yop^{51*}Δ162-catalyzed reactions of *p*NPP (closed circles) and *p*NPS (open circles). The values of K_i for arsenate for these reactions are 2.7 ± 0.1 mM and 5.8 ± 0.3 mM, respectively. The combined fit to all of the data is shown (line) and gives a value of 3.7 ± 0.5 mM. The *p*NPS concentration used in the assay was near the observed K_M, which suppresses the inhibition from arsenate, and correction for this effect using Eq. S1, gives an estimated value of K_i = 3.9 mM, in close agreement with the inhibition constant observed for the phosphatase activity.

$$K_i^{observed} = K_i(1+[S]/K_M) \quad \text{(S1)}$$

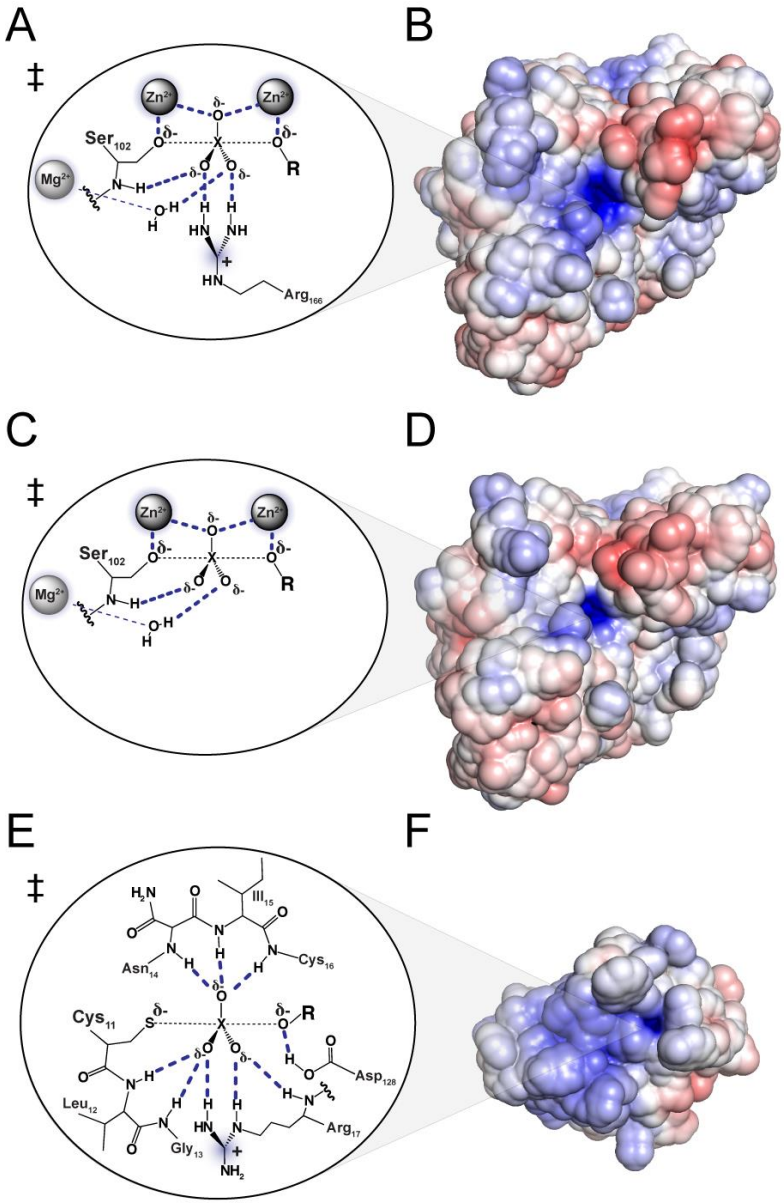

Figure S4. Comparison of the WT AP, R166S AP, and Stp1 active site and electrostatic surfaces. Active site schematic for WT AP (A), R166S AP (C), and Stp1 (E) with the expected interactions (dark blue dashes) in the transition state for phosphoryl or sulfuryl transfer from a monoester. The central phosphorus or sulfur atom is denoted by an 'X'. Model for the electrostatic surface potential for WT AP (B), R166S AP (D), and Stp1 (F). The protein surface is colored according to electrostatic potential (positive, blue; negative, red; ±6 kT/e). For the electrostatic calculation, the active site nucleophile of AP and Stp1 was deprotonated and for Stp1 the Asp28 general acid was protonated. Created with AMBER/ABPS in MacPyMOL.[18,19]

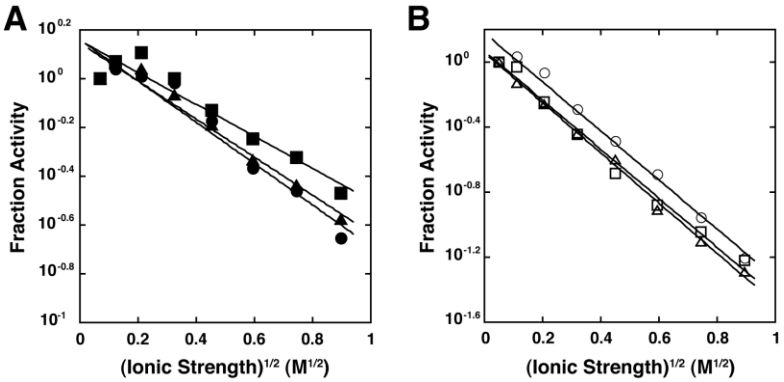

Figure S5. Ionic strength dependence of R166S AP *p*NPP hydrolysis activity (A) and Stp1 *p*NPP hydrolysis activity (B) in NaBr (circles), NaCl (triangles), or KCl (squares). For R166S AP, assays were conducted in 5 mM NaMOPS, pH 8.0 with varying concentrations of salt at 30 °C. Solid lines show best fits to the equation $log(\text{activity}) = 2A \times Z_o \times Z_{enz} \times \sqrt{I} + C$, where A is 0.516 at 30° C, C is the fraction activity as the ionic strength approaches zero, and Z_o is fixed at -2 for the *p*NPP data. The best fits yield Z_{enz} values of 0.42 ± 0.04, 0.39 ± 0.03, and 0.33 ± 0.04 for assays conducted using NaBr, NaCl, or KCl, respectively. For Stp1, assays were conducted in 5 mM NaMaleate, pH 6.0 with varying concentrations of salt at 30 °C. Solid lines show best fits yielding Z_{enz} values of 0.73 ± 0.03, 0.75 ± 0.02, and 0.73 ± 0.03 for assays conducted using NaBr, NaCl, or KCl, respectively.

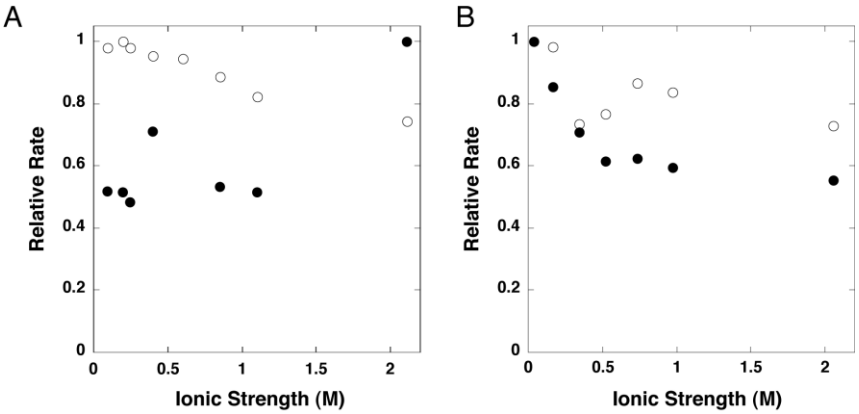

Figure S6. Uncatalyzed rates of *p*NPP (closed circles) and *p*NPS (open circles) hydrolysis versus the solution ionic strength under the assay conditions (see Methods) used for R166S (A) and Stp1 (B). Rates were normalized to the fastest rate for comparison. For (A) the fastest rate was at ionic strength 2.1 M and for (B) the fastest rate was at ionic strength 0.03 M.

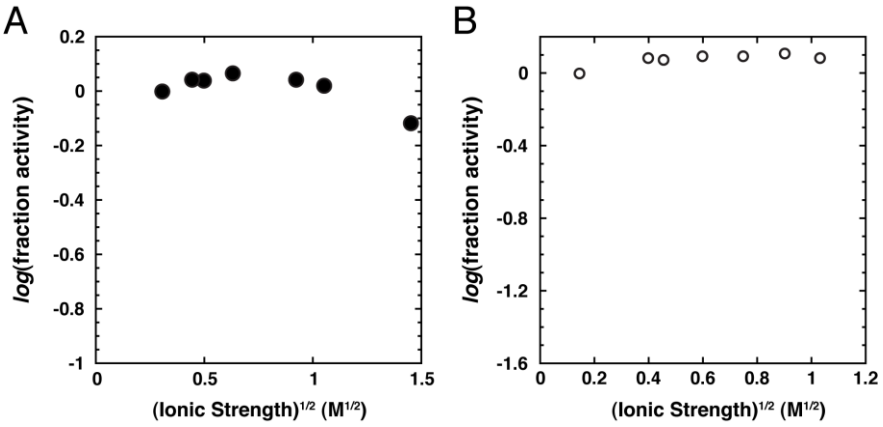

Figure S7. *p*NPP hydrolysis activity measured for R166S AP (A) and Stp1 (B) with the *p*NPP concentration 10-fold above K_M at various ionic strengths (varied with NaCl) under standard buffer conditions (see Methods). Activities were normalized to the activity observed at the lowest ionic strength for comparison.

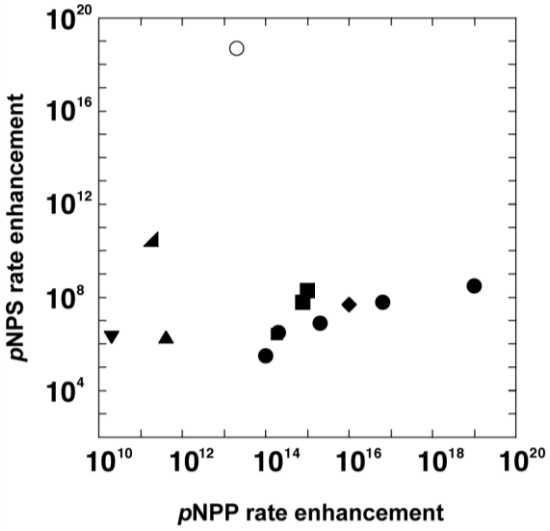

Figure S8. Plot of the enzymatic rate enhancement of *p*NPP hydrolysis with the enzymatic rate enhancement of *p*NPS hydrolysis by AP superfamily members and PTPs as in main text Figure 6 but shown here including the data point for the AP superfamily member PAS (open circle).

SUPPORTING INFORMATION REFERENCES

(1) Kirby, A.; Jencks, W. (1965) The reactivity of nucleophilic reagents toward the p-nitrophenyl phosphate dianion, J. Am. Chem. Soc. 87, 3209-3216.

(2) Benkovic, S. J.; Benkovic, P. A. (1966) Studies on sulfate esters. I. Nucleophilic reactions of amines with p-nitrophenyl sulfate, J. Am. Chem. Soc. 88, 5504-5511.

(3) O'Brien, P. J.; Herschlag, D. (2002) Alkaline phosphatase revisited: Hydrolysis of alkyl phosphates, Biochemistry 41, 3207-3225.

(4) O'Brien, P. J.; Herschlag, D. (1998) Sulfatase activity of E. coli alkaline phosphatase demonstrates a functional link to arylsulfatases, and evolutionarily related enzyme family, J. Am. Chem. Soc. 120, 12369-12370.

(5) Zalatan, J.; Fenn, T.; Brunger, A.; Herschlag, D. (2006) Structural and functional comparisons of nucleotide pyrophosphatase/ phosphodiesterase and alkaline phosphatase: Implications for mechanism and evolution, Biochemistry 45, 9788-9803.

(6) Lassila, J.; Herschlag, D. (2008) Promiscuous sulfatase activity and thio-effects in a phosphodiesterase of the alkaline phosphatase superfamily, Biochemistry 47, 12853-12859.

(7) Berlutti, F. P., C.; Selan, L.; Thaller, M. C.; Rossolini, R. M. (2001) The *Chryseobacterium meningosepticum* PafA enzyme: prototype of a new enzyme family of

prokaryotic phosphate-irrepressible alkaline phosphatases?, Microbiology 147, 2831-2839.

(8) Kim, A.; Benning, M. M.; OkLee, S.; Quinn, J.; Martin, B. M.; Holden, H. M.; Dunaway-Mariano, D. (2011) Divergence of chemical function in the alkaline phosphatase superfamily: Structure and mechanism of the P-C Bond cleaving enzyme phosphonoacetate hydrolase, Biochemistry 50, 3481-3494.

(9) Van Loo, B.; Jonas, S.; Babtie, A. C.; Benjdia, A.; Berteau, O.; Hyvonen, M.; Hollfelder, F. (2010) An efficient, multiply promiscuous hydrolase in the alkaline phosphatase superfamily, Proc. Natl. Acad. Sci. U.S.A. 107, 2740-2745.

(10) Olguin, L. F.; Askew, S. E.; O'Donoghue, A. C.; Hollfelder, F. (2008) Efficient catalytic promiscuity in an enzyme superfamily: An arylsulfatase shows a rate acceleration of 10^13 for phosphate monoester hydrolysis, J. Am. Chem. Soc. 130, 16547-16555.

(11) Nikolic-Hughes, I.; O'Brien, P.; Herschlag, D. (2005) Alkaline phosphatase catalysis is ultrasensitive to charge sequestered between the active site zinc ions, J. Am. Chem. Soc. 127, 9314-9315.

(12) Simopoulos, T. T.; Jencks, W. P. (1994) Alkaline phosphatase is an almost perfect enzyme, Biochemistry 33, 10375-10380.

(13) Hollfelder, F.; Herschlag, D. (1995) The nature of the transition state for enzyme-catalyzed phosphoryl transfer. Hydrolysis of O-aryl phosphorothioates by alkaline phosphatase, Biochemistry 34, 12255-12264.

(14) Hengge, A. C.; Edens, W. A.; Elsing, H. (1994) Transition-state structures for phosphoryl-transfer reactions of p-nitrophenyl phosphate, J. Am. Chem. Soc. 116, 5045-5049.

(15) Snyder, S. L.; Wilson, I. B. (1972) Investigations on alkaline-phosphatase catalyzed-hydrolysis of phosphoramidates. Substituent effects and transphosphorylation, Biochemistry 11, 3220-3223.

(16) Hall, A. D.; Williams, A. (1986) Leaving group dependence in the phosphorylation of *Escherichia coli* alkaline phosphatase by monophosphate esters, Biochemistry 25, 4784-4790.

(17) O'Brien, P. J.; Lassila, J. K.; Fenn, T. D.; Zalatan, J. G.; Herschlag, D. (2008) Arginine coordination in enzymatic phosphoryl transfer: Evaluation of the effect of Arg166 mutations in *Escherichia coli* alkaline phosphatase, Biochemistry 47, 7663-7672.

(18) DeLano, W. (2007) MacPyMOL: A PyMOL-based molecular graphics application for MacOS X, (DeLano Scientific LLC, Palo Alto, CA).

(19) Baker, N. A.; Sept, D.; Joseph, S.; Holst, M. J.; McCammon, J. A. (2001) Electrostatics of nanosystems: Application to microtubules and the ribosome, Proc. Natl. Acad. Sci. USA 98, 10037-10041.